Online ISSN 1848-3380, Print ISSN 0005-1144
ATKAFF 56(4), 491–498(2015)

Ivan Volarić, Nino Stojković, Saša Vlahinić

Noise and Sensitivity Improvement using SC Filters

DOI 10.7305/automatika.2016.01.1035
UDK 621.372.542.049.774

Original scientific paper

The discrete time switched capacitor (SC) based filters have number of advantages over the classical continuous time active RC based filters, the one most important being reduced circuit silicon area, allowing SC filters to be integrated to a single monolithic integrated circuit (IC). In this paper we have designed fifth order Chebyshev low pass SC filter, with a cut-off frequency $f_c = 3.4\ kHz$, and pass-band ripple $\alpha_{max} = -0.5\ dB$, and we have compared its time and frequency performance with a performance of the active RC based filter. The both SC and active RC filters are realized as a cascade of two second order sections and one first order section. All filter analysis has been performed using MATLAB and SPICE program packages where SC based filter has shown significant noise and sensitivity improvement, when compared with active RC based filter.

Key words: Low-pass filter, Filter design, Switched capacitor filter, Noise, Sensitivity

Smanjenje šuma i osjetljivosti uporabom SC filtara. Vremensko diskretni filtri s preklapanim kapacitetima imaju niz prednosti nad klasičnim vremensko kontinuiranim aktivnim RC filtrima. Jedna od važnijih prednosti jest smanjena površina silicija, omogućavajući integraciju filtra u integriranoj thenologiji (IC). U ovom radu dizajniran je Chebyshev nisko propusni filtar s preklapanim kapacitetima s graničnom frekvencijom $f_c = 3.4\ kHz$ i valovitosti $\alpha_{max} = -0.5\ dB$, te su mu vremenska i frekvencijska svojstva uspoređena sa svojstvima aktivnog RC filtra. Oba filtra realizirana su kao kaskada dviju sekcija drugog reda te jedne sekcije prvog reda. Analiza oba filtra izvršena je u MATLAB i SPICE programskim paketima, te je kod SC filtra pokazano znatno smanjenje šuma i osjetljivosti u usporedbi s aktivnim RC filtrom.

Ključne riječi: Nisko-propusni filtar, Dizajn filtra, Filtar s preklapanim kapacitetima, Šum, Osjetljivost

1 INTRODUCTION

The main motivation behind switched capacitor (SC) based circuits is to replace a resistor with a capacitor and two electric switches (usually MOS transistors) driven by the two phase non-overlapping clock [1, 2]. The time constant τ of such circuit is:

$$\tau = RC = \frac{C}{C_R}\frac{1}{f_{CL}}, \tag{1}$$

where f_{CL} is the clock frequency. Even though SC circuits have increased number of components, the overall size of the circuit is reduced since small valued capacitors can be used for acquiring desired C/C_R ratio, thus allowing the integration of the circuit into a single monolithic integrated circuit (IC). Furthermore, the C/C_R ratio can be realized with great accuracy, even up to 0.1%, while RC error can range from 20% up to 50%. In addition, since τ is dependent of f_{CL} (as shown by (1)), the cut-off frequency of SC based filters can be regulated simply by varying the clock frequency.

In this paper, we have designed switched capacitor fifth order Chebyshev low pass filter realized as a cascade of two second order sections and one first order section. Sections are based on the Sallen-Key topology, with a cut-off frequency $f_c = 3.4\ kHz$ and a pass-band ripple $\alpha_{max} = -0.5\ dB$. Through the paper we have shown significant improvement of the SC filter over the active RC filter in terms of noise and sensitivity reduction.

The paper is organized as follows. In the Section 2 we have designed and analyzed the continuous time active RC filter, while in the Section 3 we did the same with discrete time SC filter. The analysis was conducted in the frequency domain, and furthermore we investigated and compared noise and sensitivity of both filter designs.

2 CONTINUOUS TIME ACTIVE RC FILTER

The continuous time transfer function of the active RC low pass Chebyshev fifth order filter with a cut-off frequency $f_c = 3.4\ kHz$ and a pass-band ripple

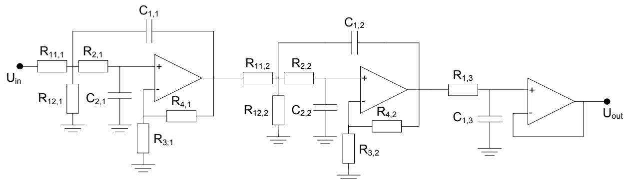

Fig. 1: The fifth order low pass active RC filter.

$\alpha_{max} = -0.5\ dB$ is given by:

$$H(s) = H_1(s) \cdot H_2(s) \cdot H_3(s), \quad (2a)$$

$$H_1(s) = \frac{4.727 \cdot 10^8}{s^2 + 4784s + 4.727 \cdot 10^8}, \quad (2b)$$

$$H_2(s) = \frac{2.176 \cdot 10^8}{s^2 + 1.252 \cdot 10^4 s + 2.176 \cdot 10^8}, \quad (2c)$$

$$H_3(s) = \frac{7740}{s + 7740}. \quad (2d)$$

The Sallen-Key topology of low pass filter is given in Fig. 1. The filter is realized as a cascade of two second order sections and one first order section. The transfer function of the given circuit is:

$$H(s) = \prod_{i=1,2} H_i(s) \cdot H_3(s), \quad (3a)$$

$$H_i(s) = \frac{(1 + \frac{G_{3,i}}{G_{4,i}})\frac{G_{11,i}G_{2,i}}{C_{1,i}C_{2,i}}}{s^2 + s(\frac{G_{1,i}+G_{2,i}}{C_{1,i}} - \frac{G_{2,i}G_{3,i}}{C_{2,i}G_{4,i}}) + \frac{G_{1,i}G_{2,i}}{C_{1,i}C_{2,i}}}, \quad (3b)$$

$$H_3(s) = \frac{\frac{1}{R_{1,3}C_{1,3}}}{s + \frac{1}{R_{1,3}C_{1,3}}}. \quad (3c)$$

Element values have been calculated by comparing equations (2a) - (2d) with (3a) - (3c) with $C_{1,i} = C_{2,i}$ and $R_{1,i} = R_{2,i}$, and are given in Table 1.

Frequency analysis of the filter is shown in Fig. 2 and 3. Calculated values are obtained from the filter transfer function (2a) - (2d), while simulated values are obtained by simulating the circuit shown in Fig. 1 with element values shown in the Table 1. The difference between the characteristics is minimal, as can be seen in zoomed inset of Fig. 2.

The equivalent circuit of the active RC filter for the calculation of the voltage noise spectral density is shown in Fig. 4. Current noise sources: $I_{n_{j,i}} = \sqrt{\frac{4kT}{R_{j,i}}}$ were added parallel to the resistors, while voltage noise sources ($E_{n_{1,i}} = 15\ nV/\sqrt{Hz}$ for LT1055) were added at input of the operational amplifiers. The operational amplifier input noise currents were neglected since their values are significantly smaller ($I_n = 1.8\ fA/\sqrt{Hz}$ for LT1055). The total voltage noise spectral density is calculated as [3]:

$$V_n^2(\omega)=\sum_{k=1}^{m} |T_{I,k}(j\omega)|^2 (I_{n,k})^2+\sum_{l=1}^{n} |T_{U,l}(j\omega)|^2 (E_{n,l})^2, \quad (4)$$

Table 1: Element values of the continuous time active RC filter shown in Fig. 1.

	1st section	2nd section	3rd section
$R_{11,i}$	$12.8\ k\Omega$	$14.6\ k\Omega$	-
$R_{12,i}$	$7.2\ k\Omega$	$12.7\ k\Omega$	-
$R_{1,i}$	-	-	$12.9\ k\Omega$
$R_{2,i}$	$4.6\ k\Omega$	$6.8\ k\Omega$	-
$R_{3,i}$	$2.6\ k\Omega$	$4.1\ k\Omega$	-
$R_{4,i}$	$4.7\ k\Omega$	$4.7\ k\Omega$	-
$C_{1,i}$	$10\ nF$	$10\ nF$	$10\ nF$
$C_{2,i}$	$10\ nF$	$10\ nF$	-

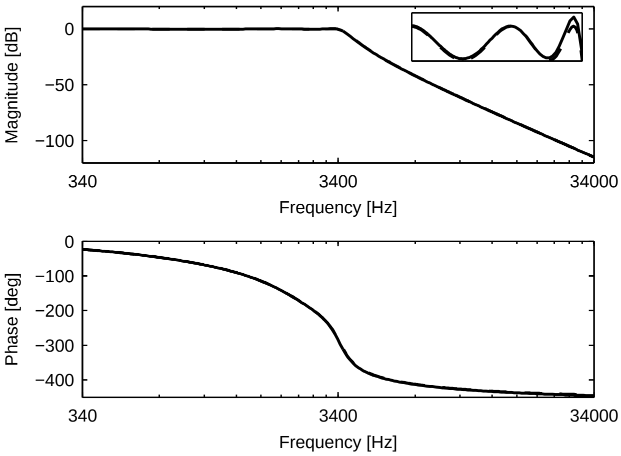

Fig. 2: Transfer function of the continuous time active RC filter: simulated (full) and calculated (dashed). Magnitude values between $f_c/100$ and f_c are zoomed in to a range from $-0.5\ dB$ to $0.2\ dB$.

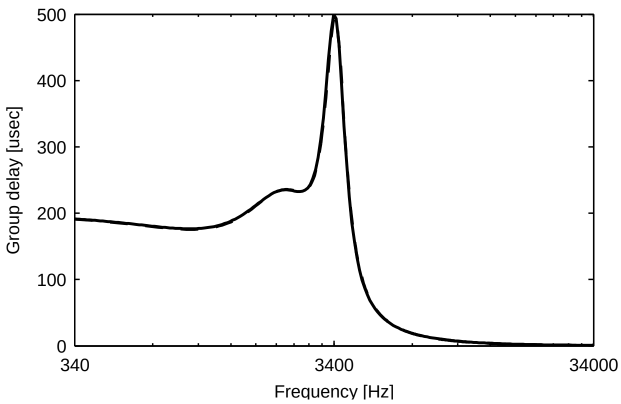

Fig. 3: Group delay of the continuous time active RC filter: simulated (full) and calculated (dashed). The values have been calculated as: $GD(\omega) = -d\varphi/d\omega$, where φ is a filter phase response.

Table 2: Section specific voltage noise transfer functions of the continuous time active RC filter.

Noise source	*Transfer function*
$\frac{U_i}{I_{n11,i}},\ i=1,2$	$\frac{R_{11,i}R_{12,i}(R_{3,i}+R_{4,i})}{s^2C_{1,i}C_{2,i}R_{11,i}R_{12,i}R_{2,i}R_{3,i}+s(C_{2,i}R_{2,i}R_{3,i}(R_{11,i}+R_{12,i})+R_{11,i}R_{12,i}(C_{2,i}R_{3,i}-C_{1,i}R_{4,i}))+R_{3,i}(R_{11,i}+R_{12,i})}$
$\frac{U_i}{I_{n12,i}},\ i=1,2$	$\frac{R_{11,i}R_{12,i}(R_{3,i}+R_{4,i})}{s^2C_{1,i}C_{2,i}R_{11,i}R_{12,i}R_{2,i}R_{3,i}+s(C_{2,i}R_{2,i}R_{3,i}(R_{11,i}+R_{12,i})+R_{11,i}R_{12,i}(C_{2,i}R_{3,i}-C_{1,i}R_{4,i}))+R_{3,i}(R_{11,i}+R_{12,i})}$
$\frac{U_i}{I_{n2,i}},\ i=1,2$	$\frac{R_{2,i}(R_{3,i}+R_{4,i})(sC_{1,i}R_{11,i}R_{12,i}+R_{11,i}+R_{12,i})}{s^2C_{1,i}C_{2,i}R_{11,i}R_{12,i}R_{2,i}R_{3,i}+s(C_{2,i}R_{2,i}R_{3,i}(R_{11,i}+R_{12,i})+R_{11,i}R_{12,i}(C_{2,i}R_{3,i}-C_{1,i}R_{4,i}))+R_{3,i}(R_{11,i}+R_{12,i})}$
$\frac{U_i}{I_{n3,i}},\ i=1,2$	$\frac{R_{3,i}R_{4,i}(s^2C_{1,i}C_{2,i}R_{11,i}R_{12,i}R_{2,i}+s(C_{2,i}R_{12,i}(R_{11,i}+R_{2,i})+R_{11,i}(C_{1,i}R_{12,i}+C_{2,i}R_{2,i}))+R_{11,i}+R_{12,i}}{s^2C_{1,i}C_{2,i}R_{11,i}R_{12,i}R_{2,i}R_{3,i}+s(C_{2,i}R_{2,i}R_{3,i}(R_{11,i}+R_{12,i})+R_{11,i}R_{12,i}(C_{2,i}R_{3,i}-C_{1,i}R_{4,i}))+R_{3,i}(R_{11,i}+R_{12,i})}$
$\frac{U_i}{I_{n4,i}},\ i=1,2$	$\frac{R_{3,i}R_{4,i}(s^2C_{1,i}C_{2,i}R_{11,i}R_{12,i}R_{2,i}+s(C_{2,i}R_{12,i}(R_{11,i}+R_{2,i})+R_{11,i}(C_{1,i}R_{12,i}+C_{2,i}R_{2,i}))+R_{11,i}+R_{12,i}}{s^2C_{1,i}C_{2,i}R_{11,i}R_{12,i}R_{2,i}R_{3,i}+s(C_{2,i}R_{2,i}R_{3,i}(R_{11,i}+R_{12,i})+R_{11,i}R_{12,i}(C_{2,i}R_{3,i}-C_{1,i}R_{4,i}))+R_{3,i}(R_{11,i}+R_{12,i})}$
$\frac{U_i}{E_{n1,i}},\ i=1,2$	$\frac{(R_{3,i}+R_{4,i})(s^2C_{1,i}C_{2,i}R_{11,i}R_{12,i}R_{2,i}+s(C_{2,i}R_{12,i}(R_{11,i}+R_{2,i})+R_{11,i}(C_{1,i}R_{12,i}+C_{2,i}R_{2,i}))+R_{11,i}+R_{12,i}}{s^2C_{1,i}C_{2,i}R_{11,i}R_{12,i}R_{2,i}R_{3,i}+s(C_{2,i}R_{2,i}R_{3,i}(R_{11,i}+R_{12,i})+R_{11,i}R_{12,i}(C_{2,i}R_{3,i}-C_{1,i}R_{4,i}))+R_{3,i}(R_{11,i}+R_{12,i})}$
$\frac{U_{out}}{I_{n1,3}}$	$\frac{R_{1,3}}{1+C_{1,3}R_{1,3}s}$
$\frac{U_{out}}{E_{n1,3}}$	1

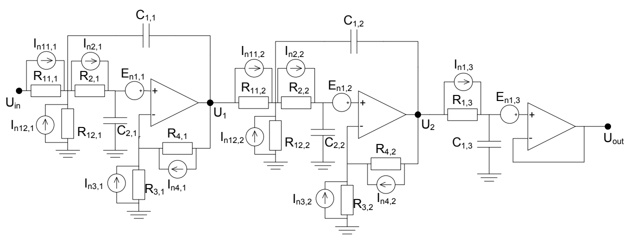

Fig. 4: Equivalent noise circuit of the continuous time active RC filter.

where $T_{I,k}$ and $T_{U,l}$ are the transfer functions of the current noise sources $I_{n,k}$ and the voltage noise sources $E_{n,l}$, respectively. Table 2 shows section specific transfer function of each noise source, and in order to get a complete transfer function, the section specific transfer function must be multiplied with transfer functions of all following sections (i.e $T_{I,1}(s) = \frac{U_{out}}{I_{n11,1}} = \frac{U_1}{I_{n11,1}}H_2(s)H_3(s)$). Figure 5 shows the total voltage noise spectral density. The small difference between calculated and simulated values can be explained with differences in noise source models. Real element noise models used in SPICE are slightly different than here used theoretical values made only from thermal noise sources. The noise RMS can be calculated as:

$$(E_n^2)_{ef} = \int_{\omega_1}^{\omega_2} V_n^2(\omega)d\omega. \tag{5}$$

In order to investigate filters sensitivity we calculated Schoeffler sensitivity as [4]:

$$I_s^2(\omega) = \sum_i (S_{x_i}^{|H(j\omega)|})^2, \tag{6}$$

where:

$$S_{x_i}^{|H(j\omega)|} = \frac{d|H(j\omega)|}{dx_i} \cdot \frac{x_i}{|H(j\omega)|}, \tag{7}$$

for each passive filter element x_i and the result is presented in Fig. 6. The multi-parameter sensitivity is defined by:

$$M = \int_{\omega_1}^{\omega_2} I_s^2(\omega)d\omega. \tag{8}$$

The Monte Carlo analysis of filter has been conducted over 100 passes with 1% element tolerance, and is shown in Fig. 7. The most significant contributions to the overall noise and sensitivity figures are presented in Figs. 8 and 9, respectively.

In order to decrease both the noise and the sensitivity, optimization algorithm described in [5] has been applied, and operational amplifier LT1055 has been replaced with low noise LT1007 operational amplifier ($E_n = 2.5\ nV/\sqrt{Hz}$). The newly calculated filter element values are shown in Table 3, while voltage noise spectral density and Schoeffler sensitivity are shown in Fig. 10 and 11, respectively. The noise RMS value is 140% smaller, while multiparameter sensitivity measure is 15% smaller, when compared to non-optimized filter values, shown in Fig. 5 and 6. Note that significant decrease of noise and sensitivity is obtained in filter pass-band.

3 DISCRETE TIME SC FILTER

The discrete time transfer function is obtained by applying forward Euler transformation ($s \Rightarrow \frac{z-1}{T_s}$, where T_S is the sampling time) to the continuous time transfer function, defined by (2a) - (2d), with sampling frequency

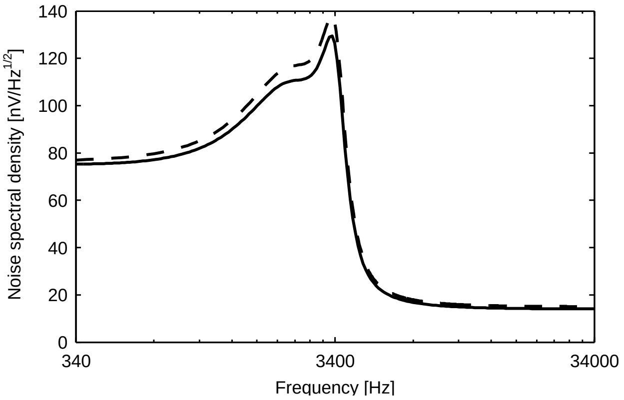

Fig. 5: Voltage noise spectral density of the continuous time active RC filter: simulated (full) and calculated (dashed). Noise RMS value is $(E_n)_{ef} = 17.595\ \mu V$ ($f_1 = 0.1 \cdot f_c$, $f_2 = 10 \cdot f_c$)

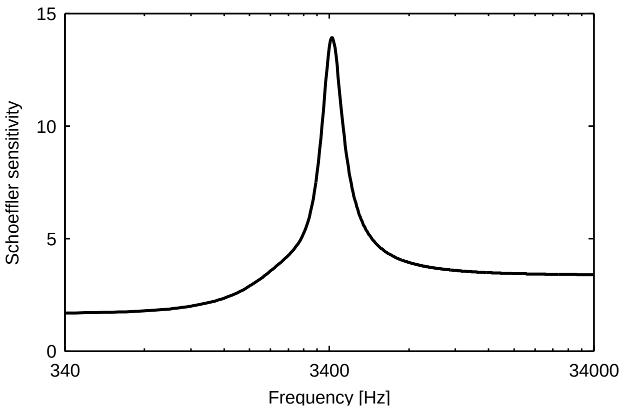

Fig. 6: Schoeffler sensitivity of the continuous time active RC filter. The multi-parameter sensitivity is $M = 8.0286 \cdot 10^5$ ($f_1 = 0.1 \cdot f_c$, $f_2 = 10 \cdot f_c$).

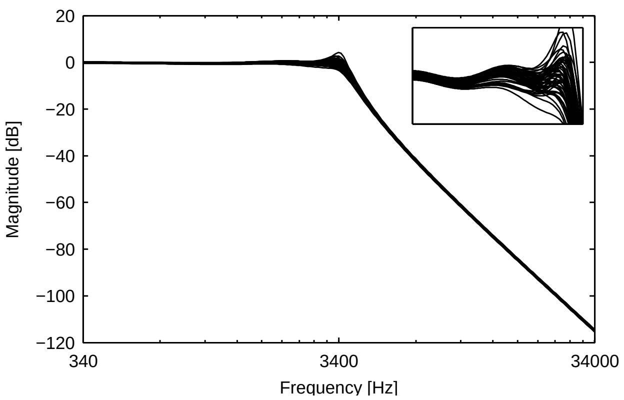

Fig. 7: Monte Carlo analysis over 100 pases with 1% element tolerance of the continuous time active RC filter. Magnitude values between $f_c/100$ and f_c are zoomed in to a range from $-3\ dB$ to $3\ dB$.

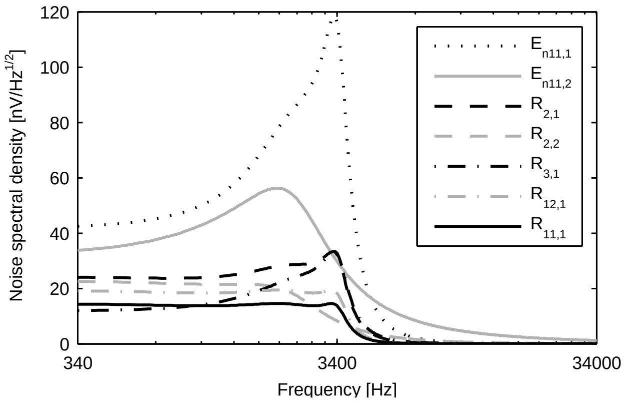

Fig. 8: Most significant contributions to the overall noise of the continuous time active RC filter.

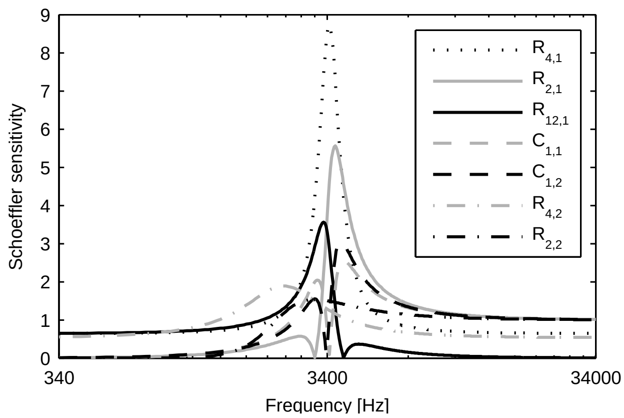

Fig. 9: Most significant contributions to the overall sensitivity of the continuous time active RC filter.

Table 3: Element values of the optimized continuous time active RC filter shown in Fig. 1.

	1st section	2nd section	3rd section
$R_{11,i}$	$12.2\ k\Omega$	$14.0\ k\Omega$	-
$R_{12,i}$	$20.9\ k\Omega$	$16.2\ k\Omega$	-
$R_{1,i}$	-	-	$12.9\ k\Omega$
$R_{2,i}$	$7.7\ k\Omega$	$7.5\ k\Omega$	-
$R_{3,i}$	$8.0\ k\Omega$	$5.4\ k\Omega$	-
$R_{4,i}$	$4.7\ k\Omega$	$4.7\ k\Omega$	-
$C_{1,i}$	$10\ nF$	$10\ nF$	$10\ nF$
$C_{2,i}$	$3.6\ nF$	$8.2\ nF$	-

$f_s = 900 f_c$:

$$H(z) = H_1(z) \cdot H_2(z) \cdot H_3(z), \tag{9a}$$

$$H_1(z) = \frac{5.048 \cdot 10^{-5}}{z^2 - 1.998z + 0.999}, \tag{9b}$$

$$H_2(z) = \frac{2.324 \cdot 10^{-5}}{z^2 - 1.996z + 0.996}, \tag{9c}$$

$$H_3(z) = \frac{0.003}{z - 0.998}. \tag{9d}$$

Figure 12 shows the electric circuit of the discrete time

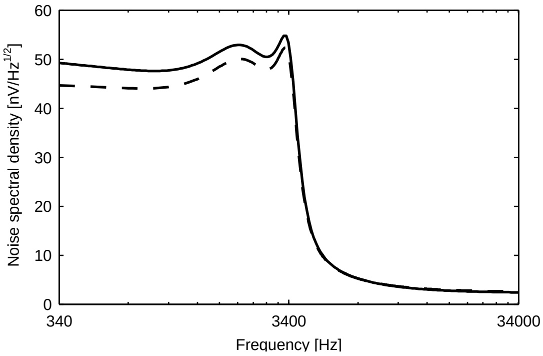

Fig. 10: Voltage noise spectral density of the optimized continuous time active RC filter: simulated (full) and calculated (dashed). Noise RMS value is $(E_n)_{ef} = 7.212\ \mu V$ ($f_1 = 0.1 \cdot f_c$, $f_2 = 10 \cdot f_c$)

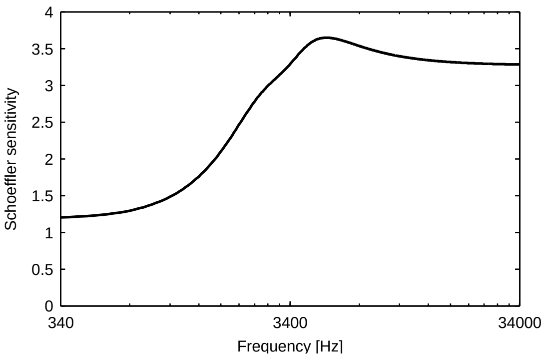

Fig. 11: Schoeffler sensitivity of the optimized continuous time active RC filter. The multi-parameter sensitivity, is $M = 6.8861 \cdot 10^5$ ($f_1 = 0.1 \cdot f_c$, $f_2 = 10 \cdot f_c$).

SC filter based on Sallen-Key topology [1]. The transfer function of the given circuit is:

$$H(z) = \prod_{i=1,2} \frac{n_{1,i}}{d_{1,i} z^2 - d_{2,i} z + d_{3,i}} \cdot \\ \cdot \frac{C_{R1,3}}{(C_{R1,3} + C_{1,3})z - C_{1,3}}, \tag{10a}$$

$$n_{1,i} = C_{R1,i} C_{R2,i} (C_{1,i} + C_{g,i}), \tag{10b}$$

$$\begin{aligned} d_{1,i} = {} & C_{2,i}[(C_{1,i} + C_{g,i})^2 + C_{R1,i}(C_{1,i} + C_{g,i})] + \\ & + C_{R2,i}[(C_{1,i} + C_{g,i})^2 + C_{R2,i}(C_{1,i} + \\ & + C_{g,i} + C_{R1,i}) + C_{2,i}(C_{1,i} + C_{g,i} + \\ & + C_{R1,i}) + C_{R1,i}(C_{1,i} + C_{g,i})], \end{aligned} \tag{10c}$$

$$\begin{aligned} d_{2,i} = {} & C_{2,i}[2(C_{1,i} + C_{g,i})^2 + C_{R1,i}(C_{1,i} + C_{g,i})] + \\ & + C_{R2,i}[(C_{1,i} + C_{g,i})^2 + C_{R2,i}(C_{1,i} + \\ & + C_{g,i} + C_{R1,i}) + C_{1,i}(C_{1,i} + C_{g,i}) + \\ & + C_{2,i}(C_{1,i} + C_{g,i} + C_{R1,i})], \end{aligned} \tag{10d}$$

$$\begin{aligned} d_{3,i} = {} & n_{1,i} - d_{1,i} + d_{2,i} = C_{2,i}(C_{1,i} + C_{g,i})^2 + \\ & + C_{1,i} C_{R2,i}(C_{1,i} + C_{g,i}). \end{aligned} \tag{10e}$$

By comparing (9a) - (9d) with (10a) - (10e) the element values of the circuit have been calculated and are shown in Table 4.

Frequency analysis of the filter is shown in Figs. 13 and 14. The values were calculated from a discrete time transfer function of the SC filter (9a) - (9d). The Z-transformation hasn't affected desired continues time designed filter specifications, as can be observed by comparing them with Fig. 2 and 3.

Equivalent circuit for the calculation of the voltage noise spectral density is based on [6], and calculated voltage noise spectral density is shown in Fig. 15. The noise RMS value, defined by (5), is over 5 times lower, when compared with continues time active RC filter, shown in Fig. 5 and over 2 times lower, when compared with optimized active RC filter, shown in Fig. 10.

Figure 16 shows Schoeffler sensitivity of the SC filter calculated by (6), while Fig. 17 shows the results of Monte Carlo analysis over 100 pases with 1% element tolerance. The multi-parameter sensitivity, obtained from (8)

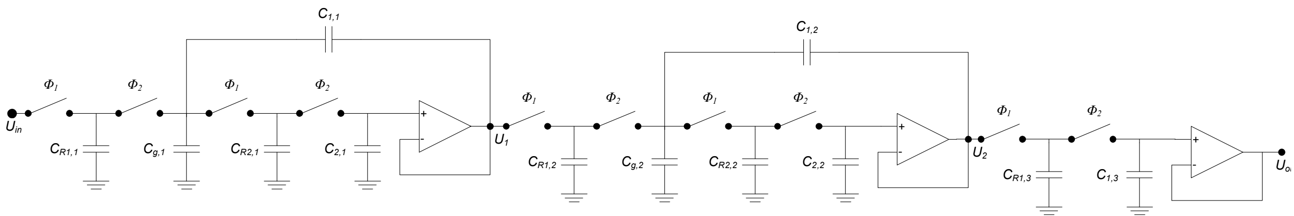

Fig. 12: The fifth order low pass SC filter.

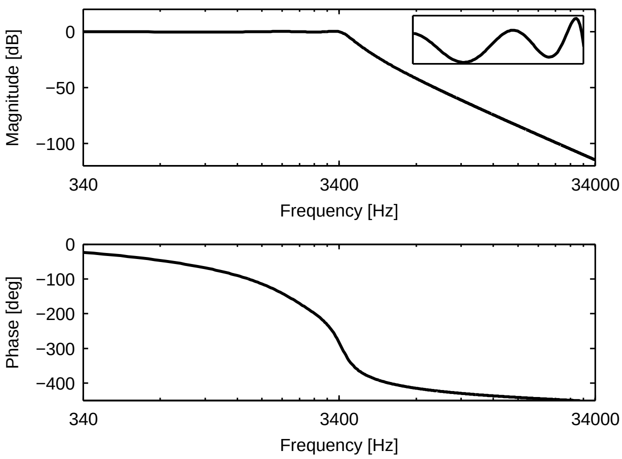

Fig. 13: Transfer function of the discrete time SC filter. Magnitude values between $f_c/100$ and f_c are zoomed in to a range from $-0.5\ dB$ to $0.3\ dB$.

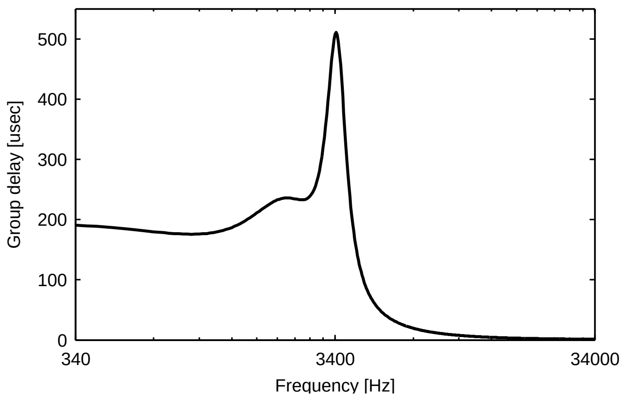

Fig. 14: Group delay of the discrete time SC filter. The values have been calculated as: $GD(\omega) = -d\varphi/d\omega$, where φ is a filter phase response.

Table 4: Element values of the discrete time SC filter shown in Fig. 12.

	1st section	2nd section	3rd section
$C_{R1,i}$	$121.1\ pF$	$1.0\ nF$	$560\ pF$
$C_{R2,i}$	$100\ pF$	$68\ pF$	-
$C_{g,i}$	$100\ pF$	$10\ nF$	-
$C_{1,i}$	$150\ nF$	$270\ nF$	$220.8\ nF$
$C_{2,i}$	$1.5\ nF$	$10.5\ nF$	-

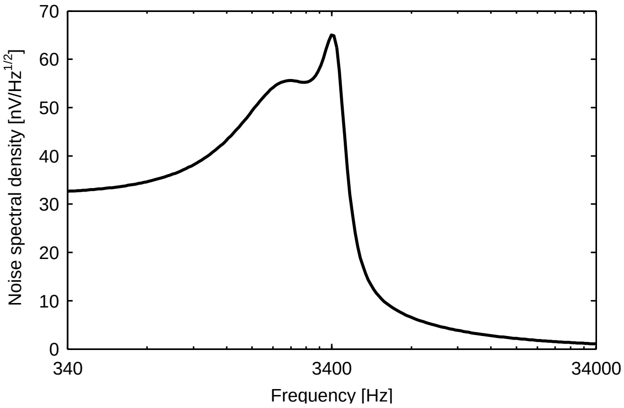

Fig. 15: Voltage noise spectral density of the discrete time SC filter. Noise RMS value is $(E_n)_{ef} = 3.129\ \mu V$ ($f_1 = 0.1 \cdot f_c$, $f_2 = 10 \cdot f_c$)

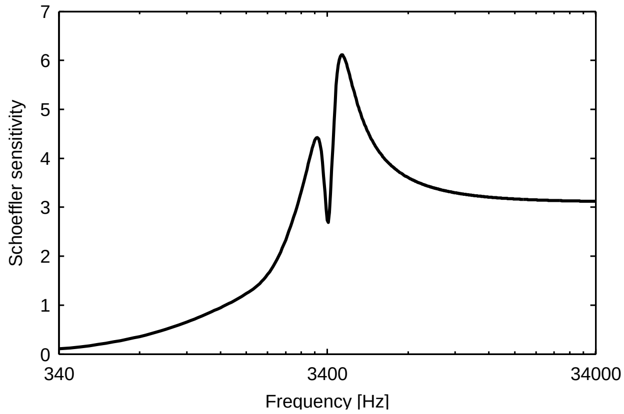

Fig. 16: Schoeffler sensitivity of the discrete time SC filter. The multi-parameter sensitivity is $M = 6.7563 \cdot 10^5$ ($f_1 = 0.1 \cdot f_c$, $f_2 = 10 \cdot f_c$).

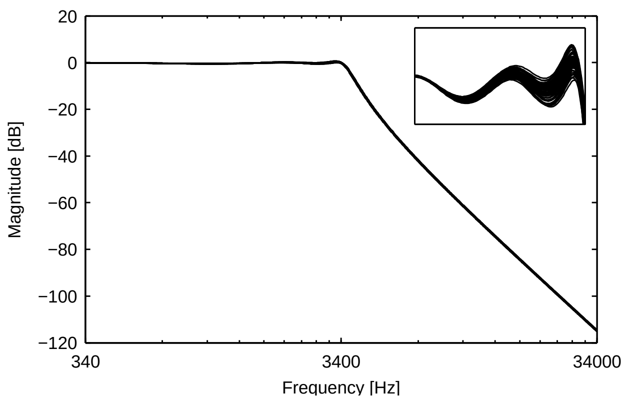

Fig. 17: Monte Carlo analysis over 100 pases with 1% element tolerance of the discrete time SC filter. Magnitude values between $f_c/100$ and f_c are zoomed in to a range from $-1\ dB$ to $1\ dB$.

is 20% smaller, and spread off the Monte Carlo analysis is significantly decreased, when compared with values obtained from continuous time active RC filter, shown in Fig. 6 and 7. The comparison of voltage noise spectral density and Schoeffler sensitivity throughout all discussed filter designs are shown in Figure 18 and 19, respectively.

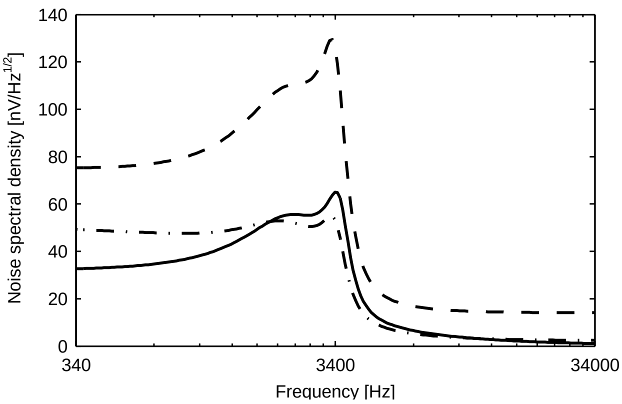

Fig. 18: Voltage noise spectral density of: active RC filter (dashed), optimized active RC filter (dot-dashed), and SC filter (full).

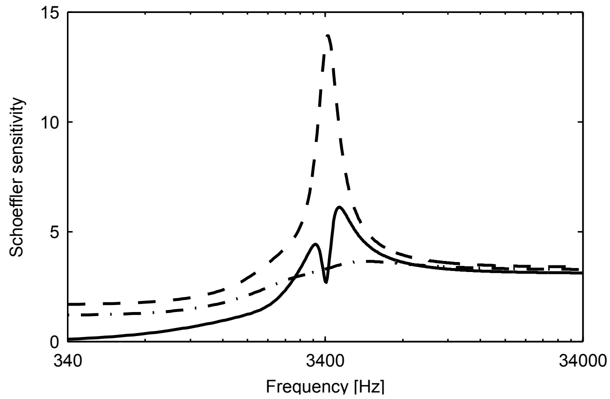

Fig. 19: Schoeffler sensitivity of: active RC filter (dashed), optimized active RC filter (dot-dashed), and SC filter (full).

4 CONCLUSION

In this paper we have shown the advantages of discrete time switched capacitor (SC) based filter over the continuous time active RC based filter by comparing their frequency performances. The filters have been designed as Chebyshev fifth order low pass filters, with a cut-off frequency $f_c = 3.4\,kHz$ and pass-band ripple $\alpha_{max} = -0.5\,dB$, and were realized as a cascade of two second order sections and one first order section, based on Sallen-Key topology. The analysis of the SC filter showed both noise and sensitivity reduction, while retaining desired frequency specifications.

Further improvement of the presented filter design can be implemented by using continuous OTA-C topology, however, this approach has its own drawbacks. Alternatively, more complex filter structure with feedbacks instead of used cascade filter structure can be used.

REFERENCES

[1] H. A. de Andrade Serra, Design of Switched-Capacitor Filters using Low Gain Amplifiers. PhD thesis, Faculdade de Ciencias e Tecnologia, Universidade Nova de Lisboa, 2012.

[2] W. K. Chen, ed., The Circuits and Filters Handbook. CRC Press, 2nd ed., 2003.

[3] M. B. J. Zurada, “Noise and dynamic range of active filters with operational amplifiers,” IEEE Transactions on Circuits and Systems, pp. 805–809, October 1975.

[4] J. D. Schoeffler, “The synthesis of minimum sensitivity networks,” IEEE Transactions on Circuit Theory, pp. 271–276, June 1964.

[5] N. Stojkovic, E. Kamenar, and M. Sverko, “Optimized second- and fourth- order LP and BP filters,” Automatika, vol. 52, no. 2, pp. 158–168, 2011.

[6] J. H. Fischer, “Noise sources and calculation techniques for switched capacitor filters,” IEEE Journal of Solid-State Circuits, vol. 17, pp. 742–752, August 1982.

Ivan Volarić was born in Rijeka, Croatia, in 1987. He received the BS, as well as MS degree in electrical engineering from the Faculty of Engineering, University of Rijeka, in 2011. Since 2012. he is a PhD student at the Faculty of Engineering, University of Rijeka. His current research interests include time-frequency signal analysis, image and video processing and statistical signal processing.

Nino Stojković received a B.Sc. degree in 1989., an M.Sc. degree in 1995 and a Ph.D. degree in 1999, all from the Faculty of Electrical Engineering and Computing, University of Zagreb. In 2012 he earned the title of professor at the Faculty of Engineering, University of Rijeka. He was a researcher on four scientific projects supported by the Croatian Ministry of Science, Education and Sports and led one scientific project. He publish several textbooks and 40 papers in magazines and conference proceedings. His research interests include analog signal processing and communication technologies. He was a Fulbright grantee for the year 2003/2004 at Texas A&M University, College Station, Texas. He was Vice Dean for education and Chair of the Department of Automation, Electronics and Computing.

Saša Vlahinić received a B.Sc. and a Ph.D. degree in Electronic Engineering from the University of Trieste, Italy, in 1998 and 2003, respectively. From 2000 to 2005 he was a junior researcher at the Department of Automation, Electronics and Computing, Faculty of Engineering, University of Rijeka, Croatia. Since 2005 he has been an Assistant Professor at the same faculty, where he teaches several courses in the field of electrical measurement and electronic instrumentation. His current research interests are in the area of filter design for measurements, distributed measurements of power quality in electric power systems, and their monitoring, control, and prediction.

AUTHORS' ADDRESSES

Ivan Volarić, mag. ing. el.,
Prof. Nino Stojković, PhD,
Prof. SašaVlahinić, PhD,
Faculty of Engineering,
University of Rijeka,
Vukovarska 58, 51000 Rijeka,
HR - Croatia,
e-mail: ivolaric@riteh.hr, nino.stojkovic@riteh.hr, sasa.vlahinic@riteh.hr

Received: 2014-10-03
Accepted: 2015-10-22